SOLVING 3D PROBLEMS OF POTENTIAL THEORY IN PIECEWISE HOMOGENEOUS MEDIA BY USING INDIRECT BOUNDARY AND NEAR-BOUNDARY ELEMENT METHODS

Liubov Zhuravchak, Olena Kruk
Lviv Polytechnic National University, Ukraine
lzhuravchak@ukr.net, olena0306@gmail.com

Abstract: Effective numerical-analytical approaches for solving the direct problem of electrical prospecting for the media with inclusions of arbitrary shape and constant electrical characteristics are suggested. They are based on the combination of a fundamental solution of Laplase's equation and principal ideas of the method of boundary integral equations and that of collocation.

Using the indirect boundary and near-boundary element methods, numerical-analytical approaches for solving the problems of potential theory in spatial piecewise homogeneous objects under conditions of an ideal contact between their components are developed. Discrete-continuous models for finding the intensities of unknown sources introduced into the boundary and near-boundary elements, and approximated by constants are reduced to the systems of linear algebraic equations resulted from the satisfaction, in a collocation sense, of the boundary conditions and those of an ideal interface contact.

The software implementation of the approaches proposed in a half-space with inclusions of various shapes and electrical conductivity for the electrical profiling method in a 3D problem of dc electrical prospecting is done. The numerical analysis performed for some mathematical models illustrates high accuracy and potential abilities of the methods suggested. The developed algorithms make it possible to calculate the potential and intensity of an electric field in inhomogeneous media which are characterized by nonplanar boundaries and arbitrary, by depth and lateral distribution, stationary current sources.

An influence of conductivity and depths of inclusions, their shapes, a distance between two spherical inclusions on the apparent resistivity calculated by the difference of potentials measured on a half-space surface is investigated. It is shown that information on a potential field obtained on the surface of the object can be used to identify local foreign inclusions.

The proposed approaches could be the basis for solving inverse problems of geophysics and technical diagnostics in developing methods for the identification of foreign inclusions, voids and defects, and determining their conductivity, dimentions, and location.

Key words: indirect boundary element method, indirect near-boundary element method, piecewise homogeneous medium, electrical profiling method, 3D problems of potential theory.

1. Introduction

Considering as many physical properties of inhomogeneous continuous media and potential fields acting in the media as possible allows the researchers to study their structure in the best possible way. Mathematical models for the distribution of stationary fields of various physical nature (thermal, diffusion, direct current) in three-dimensional piecewise homogeneous media are based on solving boundary problems for the systems of elliptic equations. The development of effective numerical-analytical approaches to solving these problems is of considerable applied interest both for engineering and for various applications, in particular in geophysics, as this enables us to estimate the intensity of these fields quantitatively, and consider their interaction.

At every stage of the prospecting investigation, from desining and choosing rational observation systems to interpreting field data, the possibility of mathematical modelling of real situations is of particular importance. Under the existing conditions, solving the direct and inverse problems of prospecting often employs a theoretical analysis of an electric field in complex geoelectric sections by means of mathematical modelling and computer facilities. Analytical solutions to such problems for inhomogeneous media were obtained by using Green's functions only for particular cases when the inclusions are of canonic form. The application of the method of finite differences and the one of finite elements to study electric fields is complicated by inaccuracy of the models' description, especially in the case of infinite or half-infinite objects.

In this connection, for inhomogeneous media we find it expedient to use the ideas and schemes of systhesis of a new effective numerical-analytical technique [1] based on the principles of decomposition and composition, and take into account the advantages of

different methods. We propose a technique of numerical solution of a 3D direct problem of electrical prospecting by a direct current in complex geoelectric sections with arbitrary, in particular nonplanar, media interfaces. It is based on the simultaneous application of the method of boundary integral equations [2–5], which facilitates the description of a half-infinite domain, and the near-boundary element method [1] in which the integral equations are written in the outer near-boundary zone of the solution domain (unlike the boundary element method with integral equations on the domain boundary).

2. Developing a mathematical model

Consider an object $\Omega \subset \mathbf{R}^3$ consisting of M domains: $\Omega = \cup_{m=1}^{M}(\Omega_m \cup \Gamma_m)$ where Γ_m is the boundary of the domain Ω_m in the Cartesian coordinate system x_1, x_2, x_3.

Assume that the unknown variable (temperature, electric or magnetic field potencial) $q^{(m)}(x)$ $(m=1,...,M)$ satisfies the equation

$$\mathbf{P}_0^{(m)}(q^{(m)}(x)) = \Delta q^{(m)}(x) = -y^{(m)}(x), x \in \Omega_m,$$
$$\Omega_m \subset \mathbf{R}^3, m=1,...,M \tag{1}$$

with the given boundary conditions:

$$q^{(m)}(x) = f_\Gamma^{(1)}(x), x \in \partial\Omega^{(1)}, \tag{2}$$

$$-l_{0m}\frac{\partial q^{(m)}(x)}{\partial \mathbf{n}^{(m)}(x)} = f_\Gamma^{(2)}(x), x \in \partial\Omega^{(2)}, \tag{3}$$

$$-l_{0m}\frac{\partial q^{(m)}(x)}{\partial \mathbf{n}^{(m)}(x)} + u(x)q^{(m)}(x) = u(x)f_\Gamma^{(3)}(x),$$
$$x \in \partial\Omega^{(3)}. \tag{4}$$

and the conditions of an ideal contact at the media interface:

$$q^{(m)}(x) = q^{(s)}(x), x \in \Gamma^{ms}, \ s > m, s \in \{2,...,M\}, \tag{5}$$

$$l_{0m}\frac{\partial q^{(m)}(x)}{\partial \mathbf{n}^{(m)}(x)} = l_{0s}\frac{\partial q^{(s)}(x,t)}{\partial \mathbf{n}^{(s)}(x)},$$
$$x \in \Gamma^{ms}, s > m, s \in \{2,...,M\}. \tag{6}$$

Here Ω_m is the homogeneous domain with a/ constant characteristic l_{0m}; $y^{(m)}(x)$ is the intensity of the determined inner sources in the domain Ω_m; $\mathbf{n}^{(m)}(x) = (\mathbf{n}_1^{(m)}(x), \mathbf{n}_2^{(m)}(x), \mathbf{n}_3^{(m)}(x))$ is the vector of an outer uniquely determined normal to $\P\Omega_m$; $\Gamma^{ms} = \partial\Omega_m \cap \partial\Omega_s$ is the media interface of Ω_m and Ω_s; $u(x)$ is the coefficient, which characterizes the object surface; $f_\Gamma^{(j)}(x)$ are the known functions.

3. Integral representations of solutions to equations, and boundary integral equation system (BIES)

To develop an algorithm for solving problem (1)–(6), let us now consider the set $\mathbf{R}^3(M)$ that is composed of the spaces $\mathbf{R}_m^3$ and owns the following properties [1]:

$$\mathbf{R}_m^3 \cap \mathbf{R}^3 = \Omega_m \cup \Gamma_m, \mathbf{R}_m^3 \cap \mathbf{R}_s^3 = \Gamma^{ms},$$
$$\mathbf{R}^3(M) \cap \mathbf{R}^3 = \Omega \cup \Gamma. \tag{7}$$

According to the indirect near-boundary element method (INBEM) [1, 6-8, 10], let us introduce the outer near-boundary domains $G_m = B_m \setminus \Omega_m$ ($\Omega_m \subset B_m \subset \mathbf{R}_m^3$, $\Gamma_m \cap \partial B_m = \varnothing$, ∂B_m is the domain boundary of B_m) with the unknown functions $j^{(Gm)}(x)$ which describe the distribution of fictitious sources. Similarly, according to the indirect boundary element method (IBEM) [2], on the boundaries of Γ_m, let us introduce the unknown functions $j^{(\Gamma m)}(x)$. The domain of defining the functions $q^{(m)}(x)$ having been extended for the whole $\mathbf{R}_m^3$, from (1), we obtain

$$\mathbf{P}_0^{(m)}(q^{(gm)}(x)) = -j^{(gm)}(x)c_{gm} - y^{(m)}(x)c_m, x \in \mathbf{R}_m^3, \tag{8}$$

where $g \in \{\Gamma, G\}$, c_m, c_{gm} are the characteristic functions of Ω_m, g_m equal to one within these domains and to zero on and outside their boundaries.

As for the operator $\mathbf{P}_0^{(m)}(q^{(m)}(x))$ there exists a known fundamental solution $U^{(m)}(x,x)$, then the integral representations of the unknown potentials as the solutions to equation system (8) and their derivatives with respect to the normal are of the following form [1, 2]:

$$q^{(gm)}(x) = \mathbf{F}^{(gm)}(x, U^{(m)}) + b^{(m)}(x, U^{(m)}), \tag{9}$$

$$-l_{0m}\frac{\partial q^{(gm)}(x)}{\partial \mathbf{n}^{(m)}(x)} = \mathbf{F}^{(gm)}(x, Q^{(m)}) + b^{(m)}(x, Q^{(m)}), \tag{10}$$

where

$$\mathbf{F}^{(gm)}(x, \Phi^{(m)}) = \int\limits_{g_m} \Phi^{(m)}(x,x)j^{(gm)}(x)dg_m(x), \tag{11}$$

$$b^{(m)}(x, \Phi^{(m)}) = \int\limits_{\Omega_m} \Phi^{(m)}(x,x)y^{(m)}(x)d\Omega_m(x), \tag{12}$$

$U^{(m)}(x,x^{(m)})$ is the fundamental solution (FS) to the Laplace operator which exactly satisfies equation (8) in Ω_m:

$$U^{(m)}(x,x^{(m)}) = \frac{1}{4pl_{0m}r_m},$$

$$r_m = \sqrt{\sum_{l=1}^{3}(x_l - x_l^{(m)})^2}, \Phi^{(m)} \in \{U^{(m)}, Q^{(m)}\}, \tag{13}$$

$$Q^{(m)}(x,x^{(m)}) = -l_{0m}\frac{\partial U^{(m)}(x,x^{(m)})}{\partial \mathbf{n}^{(m)}(x)} = -l_{0m} \times \tag{14}$$

$$\times \sum_{l=1}^{3}\frac{\partial U^{(m)}(x,x^{(m)})}{\partial x_i}\mathbf{n}_l^m(x) = \sum_{l=1}^{3}\frac{(x_l - x_l^{(m)})\mathbf{n}_l^m(x)}{4pr^3}$$

$$x^{(m)} = (x_1^{(m)}, x_2^{(m)}, x_3^{(m)}) \in \mathbf{R}_m^3.$$

Directing x from the middle of the domain Ω_m to the boundary Γ_m, instead of (9) we obtain a BIES which links the unknown functions $j^{(gm)}(x)$ with the known ones $y^{(m)}(x)$, and $f_\Gamma^{(1)}(x)$, $f_\Gamma^{(2)}(x)$, $f_\Gamma^{(3)}(x)$ in order to satisfy boundary conditions (2)-(4):

$$\mathbf{F}^{(gm)}(x,U^{(m)}) = f_\Gamma^{(1)}(x) - b^{(m)}(x,U^{(m)}),$$
$$x \in \P\Omega^{(1)} \tag{15}$$

$$-\frac{1}{2}j^{(\Gamma m)}(x) + \mathbf{F}^{(\Gamma m)}(x,Q^{(m)}) = \tag{16}$$
$$= f_\Gamma^{(2)}(x) - b^{(m)}(x,Q^{(m)}), \quad x \in \P\Omega^{(2)}$$

or

$$\mathbf{F}^{(Gm)}(x,Q^{(m)}) = f_\Gamma^{(2)}(x) - b^{(m)}(x,Q^{(m)}),$$
$$x \in \P\Omega^{(2)}, \tag{17}$$

$$-\frac{1}{2}f^{(\Gamma m)}(x) + \mathbf{F}^{(\Gamma m)}(x,Q^{(m)} + u(x)U^{(m)}) = \tag{18}$$
$$u(x)f_\Gamma^{(3)}(x) - b^{(m)}(x,Q^{(m)} + u_{0m}U^{(m)}), x \in \P\Omega^{(3)},$$

or

$$\mathbf{F}^{(Gm)}(x,Q^{(m)} + u(x)U^{(m)}) = u(x)f_\Gamma^{(3)}(x)$$
$$-b^{(m)}(x,Q^{(m)} + u_{0m}U^{(m)}), \quad x \in \P\Omega^{(3)}, \tag{19}$$

and contact conditions:

$$\mathbf{F}^{(gm)}(x,U^{(m)}) - \mathbf{F}^{(gs)}(x,U^{(s)}) = -b^{(m)}(x,U^{(m)}) +$$
$$+b^{(s)}(x,U^{(s)}), x \in \Gamma^{ms}, s > m, s \in \{2,...,M\} \tag{20}$$

$$-\frac{1}{2}f^{(\Gamma m)}(x) + \mathbf{F}^{(\Gamma m)}(x,Q^{(m)}) + \frac{1}{2}f^{(\Gamma m)}(x)$$
$$-\mathbf{F}^{(\Gamma s)}(x,Q^{(s)}) = -b^{(m)}(x,Q^{(m)}) + b^{(s)}(x,Q^{(s)}), \tag{21}$$
$$x \in \Gamma^{ms}, s > m, s \in \{2,...,M\}.$$

or

$$\mathbf{F}^{(Gm)}(x,Q^{(m)}) + \mathbf{F}^{(Gs)}(x,Q^{(s)}) = -b^{(m)}(x,Q^{(m)}) -$$
$$-b^{(s)}(x,Q^{(s)}), \tag{22}$$
$$x \in \Gamma^{ms}, s > m, s \in \{2,...,M\}.$$

Note that when solving the problem using the IBEM we have BIES (15), (16), (18), (20), (21), where the integrals on the boundary from FS (13) are considered in the Riemann terms, and those from FS (14) are considered in the Cauchy terms. However, when solving the problem using the INBEM, we have BIES (15), (17), (19), (20), (22), where all the integrals in the near-boundary domain are considered in the Riemann terms [6–8].

4. Developing a discrete-continuous model

The analytical integration in BIES (15), (16), (18), (20), (21) and (15), (17), (19), (20), (22) for applied problems being practically impossible to perform due to arbitrariness of the domain Ω, and functions $j^{(m)}(x)$ and $y^{(m)}(x)$, we perform a spatial discretization in the following way.

The boundaries Γ_m and corresponding near-boundary domains G_m are discretized on V_m of boundary and near-boundary elements g_{mv}, respectively. Then $\cup_{v=1}^{V_m}g_{mv} = g_m$; Γ_{mv}, G_{mv} are the ermit elements of the second order which do not cross each other [3],

$$\cup_{v=1}^{K_{1m}}(\P G_{mv} \cap \Gamma) = \P\Omega^{(1)},$$

$$\cup_{v=K_{1m}+1}^{K_{1m}+K_{2m}}(\P G_{mv} \cap \Gamma) = \P\Omega^{(2)},$$

$$\cup_{v=K_{1m}+K_{2m}+1}^{K_m}(\P G_{mv} \cap \Gamma) = \P\Omega^{(3)},$$

$$\cup_{v=K_m+1}^{K_m + \sum_{s>m}V_{ms}}(\P G_{mv} \cap \Gamma^{ms}) = \cup_{s>m}\Gamma^{ms}$$

$$\cup_{v=1}^{K_{1m}}\Gamma_{mv} = \P\Omega^{(1)}, \quad \cup_{v=K_{1m}+1}^{K_{1m}+K_{2m}}\Gamma_{mv} = \P\Omega^{(2)},$$

$$\cup_{v=K_{1m}+K_{2m}+1}^{K_m}\Gamma_{mv} = \P\Omega^{(3)},$$

$$\cup_{v=K_m+1}^{K_m + \sum_{s>m}V_{ms}}\Gamma_v^{ms} = \cup_{s>m}\Gamma^{ms}, \; mes\, G_{mv} = 3,$$

∂G_{mv} is the boundary of the near-boundary elements G_{mv}. It is clear that each boundary element should completely belong to one of the areas $\P\Omega^{(s)}$ ($s = 1, 2, 3$), Γ^{ms} which are discretized into $\sum_m K_{sm}$, V_{ms} of the elements, respectively. The elements numbering begins from the first area and continues on the next ones, i.e. $V_m = K_m + \sum_{s>m}V_{ms}$, $K_m = K_{1m} + K_{2m} + K_{3m}$. In the boundary and near-boundary elements, the unknown functions $j_v^{(gm)}(x)$ are approximated by the

constants d_v^{gm}. The domains Ω_{my} are discretized into the elements Ω_{myq} $(q=1,...,Q_m)$.

After the 3D discretization, operators (11), (12) are given by

$$\mathbf{F}^{gm}(x,\Phi^{(m)}) = \sum_{v=1}^{V_m} A_v^{gm}(x,\Phi^{(m)})d_v^{gm},\qquad(23)$$

$$b^{(m)}(x,\Phi^{(m)}) = \sum_{q=1}^{Q_m} \int_{\Omega_{mq}} \Phi^{(m)}(x,\boldsymbol{x})y^{(m)}(\boldsymbol{x})d\Omega_{mq}(\boldsymbol{x})\quad(24)$$

where $A_v^{gm}(x,\Phi) = \int_{g_v^m} \Phi(x,\boldsymbol{x})dg_v^m(\boldsymbol{x})$.

5. Systems of linear algebraic equations (SLAEs) for finding unknown intensity sources introduced into boundary and near-boundary elements

The unknown constants d_v^{gm} are found from the SLAEs obtained from BIESes (15), (16), (18), (20), (21) and (15), (17), (19), (20), (22). The collocation points are chosen in the middle of each boundary element element)

$$\Gamma_{mw} = \P G_{mw} \cap \Gamma^m, \quad w=1,...,V_m, \cup_{w=1}^{V_m} \Gamma_{mw} = \Gamma_m.$$

Let us write down the SLAE taking into account (23), (24):

$$\sum_{v=1}^{V_m} A_v^{gm}(x^{mw},U^{(m)})d_v^{gm} = f_\Gamma^{(1)}(x^{mw}) -$$
$$-b^{(m)}(x^{mw},U^{(m)}),\qquad(25)$$
$$x^{mw} \in \partial\Omega^{(1)}, w=1,...,K_{1m},$$

$$-\frac{1}{2}d_w^{\Gamma m} + \sum_{v=1}^{V_m} A_v^{gm}(x^{mw},Q^{(m)})d_v^{gm} = f_\Gamma^{(2)}(x^{mw}) -$$
$$-b^{(m)}(x^{mw},Q^{(m)}),\qquad(26)$$
$$x^{mw} \in \partial\Omega^{(2)}, w=K_{1m}+1,...,K_{1m}+K_{2m},$$

or

$$\sum_{v=1}^{V_m} A_v^{Gm}(x^{mw},Q^{(m)})d_v^{Gm} =$$
$$= f_\Gamma^{(2)}(x^{mw}) - b^{(m)}(x^{mw},Q^{(m)}),\qquad(27)$$
$$x^{mw} \in \partial\Omega^{(2)}, w=K_{1m}+1,...,K_{1m}+K_{2m},$$

$$-\frac{1}{2}d_w^{\Gamma m} + \sum_{v=1}^{V_m} A_v^{gm}(x^{mw},Q^{(m)} +$$
$$+u(x^{mw})U^{(m)})d_v^{gm} = u(x^{mw})f_\Gamma^{(3)}(x^{mw}) -\qquad(28)$$
$$-b^{(m)}(x^{mw},Q^{(m)} +u(x^{mw})U^{(m)}),$$
$$x^{mw} \in \partial\Omega^{(3)}, w=K_{1m}+K_{2m}+1,...,K_m,$$

or

$$\sum_{v=1}^{V_m} A_v^{Gm}(x^{mw},Q^{(m)} +u(x^{mw})U^{(m)})d_v^{Gm} =$$
$$= u(x^{mw})f_\Gamma^{(3)}(x^{mw}) -\qquad(29)$$
$$-b^{(m)}(x^{mw},Q^{(m)} +u(x^{mw})U^{(m)}),$$
$$x^{mw} \in \partial\Omega^{(3)}, w=K_{1m}+K_{2m}+1,...,K_m$$

and contact conditions:

$$\sum_{v=1}^{V_m} A_v^{gm}(x^{mw},U^{(m)})d_v^{gm} - \sum_{v=1}^{V_s} A_v^{gs}(x^{mw},U^{(s)})d_v^{gs}] =$$
$$= b^{(s)}(x^{mw},U^{(s)}) - b^{(m)}(x^{mw},U^{(m)}),\qquad(30)$$
$$x^{mw} \in \partial\Omega^{ms}, w=K_m+1,...,K_m+\sum_{s>m}V_{ms},$$

$$-\frac{1}{2}d_w^{\Gamma m} + \sum_{v=1}^{V_m} A_v^{\Gamma m}(x^{mw},Q^{(m)})d_v^{\Gamma m} +\frac{1}{2}d_w^{\Gamma s} -$$
$$-\sum_{v=1}^{V_s} A_v^{\Gamma s}(x^{mw},Q^{(s)})d_v^{\Gamma s} =\qquad(31)$$
$$= b^{(s)}(x^{mw},Q^{(s)}) - b^{(m)}(x^{mw},Q^{(m)}),$$
$$x^{mw} \in \partial\Omega^{ms}, w=K_m+1,...,K_m+\sum_{s>m}V_{ms}$$

or

$$\sum_{v=1}^{V_m} A_v^{Gm}(x^{mw},Q^{(m)})d_v^{Gm} - \sum_{v=1}^{V_s} A_v^{Gs}(x^{mw},Q^{(s)})d_v^{Gs} =$$
$$= -b^{(s)}(x^{mw},Q^{(s)}) - b^{(m)}(x^{mw},Q^{(m)}),\qquad(32)$$
$$x^{mw} \in \partial\Omega^{ms}, w=K_m+1,...,K_m+\sum_{s>m}V_{ms}.$$

Next, let us develop a discrete-continuous model to determine the unknown function $q^{(m)}(x)$ and its derivative with respect to the normal both at the inner points of each Ω_m, and on the media interfaces because after finding the unknown constants d_v^{gm} from systems (25), (26), (28), (30), (31) and (25), (27), (29), (30), (32), all the domains Ω_m are considered as the completely independent ones. We shall have:

$$q^{(gm)}(x^{mz}) = \sum_{v=1}^{V_m} A_v^{gm}(x^{mz},U^{(m)})d_v^{gm} +$$
$$+b^{(m)}(x^{mz},U^{(m)}), x^{mz} \in \mathbf{Z}_m,\qquad(33)$$

$$-l_{0m}\frac{\partial q^{(gm)}(x^{mz})}{\partial \mathbf{n}^{(m)}(x)} = \sum_{v=1}^{V_m} A_v^{gm}(x^{mz},Q^{(m)})d_v^{gm} +$$
$$+b^m(x^{mz},Q^{(m)}),\qquad(34)$$

where $\mathbf{Z}_m$ are the sets of the observation points $x^z \in \Gamma_m \cup \Omega_m$.

6. Software implementation of the approach proposed in a piecewise homogeneous half-space in modelling dc prospecting problems

The proposed approach is implemented in modelling a dc profiling method in a half-space containing one or two foreign inclusions chosen in the form of spheres with a radius $R = 1$, and 2 by 2 by 2 cubes.

If we assume that the surface

$$\partial\Omega = \{(x_1, x_2, x_3) :- \infty < x_1 < \infty, - \infty < x_2 < \infty, \\ x_3 = 0\}$$

of the half-space

$$\mathbf{R}^{3-} = \{(x_1, x_2, x_3) :- \infty < x_1 < \infty, - \infty < x_2 < \infty, \\ - \infty < x_3 < 0\}$$

is electrically insulated, the problem is considerably simplified/ owing to the use of a special fundamental solution (SFS or Green's function) $U_h^{(1)}(x, \xi^{(1)})$ to Laplace's equation which satisfies automatically a zero second-kind boundary condition of the second kind:

$$\frac{\partial\theta^{(1)}(x)}{\partial n^{(1)}(x)} = 0, \quad x \in \partial\Omega. \tag{35}$$

The inclusions were in ideal electric contact with the geoenvironment. The problem was solved by using the IBEM.

The SLAE included only the equations which satisfied contact conditions (5), (6).

Problem 1. *Research into the spatial discretization of the model.*

In case of one inclusion, the SLAE for finding the unknown sources introduced into the boundary elements looks like:

$$\sum_{v=1}^{V} A_v^{\Gamma 1}(x^{1w}, U_h^{(1)}) d_v^{\Gamma 1} - \sum_{v=1}^{V} A_v^{\Gamma 2}(x^{1w}, U^{(2)}) d_v^{\Gamma 2} = \\ = b^2(x^{1w}, U^{(2)}) - b^1(x^{1w}, U_h^{(1)}), \\ w = 1,...,V, \tag{36}$$

$$\sum_{v=1}^{V_1} A_v^{\Gamma 1}(x^{1w}, Q_h^{(1)}) d_v^{\Gamma 1} - \sum_{v=1}^{V_2} A_v^{\Gamma 2}(x^{1w}, Q^{(2)}) d_v^{\Gamma 2} = \\ = b^2(x^{1w}, Q^{(2)}) - b^1(x^{1w}, Q_h^{(1)}), \\ x^{1w} \in \Gamma_2, w = 1,...,V, \tag{37}$$

where $V = V_{12} = V_2$, $\xi^{(1)\prime}$ is the mirroring of the point $\xi^{(1)}$ relative to the half-space boundary.

Since one of the main types of field observations for the direct current methods is electrical profiling with the use of the method of median gradients, with the apparent resistivity being calculated by the formula below:

$$\rho_a = \frac{k_u}{I} \left| \theta(x^M) - \theta(x^N) \right|. \tag{38}$$

Here, k_u is the installation coefficient [9], in particular,

$$k_u = 2\pi \left(\frac{1}{R_{AM}} - \frac{1}{R_{AN}} - \frac{1}{R_{BM}} + \frac{1}{R_{RN}} \right)^{-1} \quad \text{is the}$$

coefficient for an ordinary gradient installation;

$$R_{CD} = \left[\sum_{i=1}^{3} \left(x_i^C - x_i^D \right)^2 \right]^{1/2}; \quad x^C = (x_1^C, x_2^C, x_3^C) \text{ are the}$$

coordinates of the point C; A and B are the points on $\partial\Omega$, at which there were placed real direct current sources (feeding electrodes) with a power of +1 and -1; M and N are the mobile observation units (receiving electrodes) on $\partial\Omega$, between which the potential difference was determined with a measurement step of 0.04, I is the electric current intensity equal to 1. Using the coefficient k_u one can calculate the value of an apparent resistivity and plot curves based on the data resulted from the spatial model observations in the same way as those based on the field measurements.

To estimate a discretization error occurring when solving the given problem, we considered a half-space with the feeding electrodes at A(-10, 0, 0) and B(10, 0, 0) with one inclusion of the same conductivity ($\sigma_1 = \sigma_2 = 1$) placed at different depths. Note that σ_1, σ_2 ($\sigma_i = 1/\rho_i$, ρ_i is the specific electrical resistance) are used here instead of λ_1, λ_2 introduced before because they are accepted by specialists for dc prospecting problems.

The graphs given in Fig. 1 provide the possibility to estimate the error occurring when solving the given problem. The computational error proved to be between 0.3 % (Fig. 1, *a*) and 5% (Fig. 1, *b*) when changing the depth from 1.5 to 1.3, i.e. with the inclusion approaching the surface, it goes up (It is obvious that the exact result in this case is a straight line equal to 1).

It is shown that the numerical results of the problem for the electrically insulated/ inclusion ($\sigma_2 = 0$, Fig. 2, *a*) coincide with the solution to a similar problem for a homogeneous half-space containing a void with a second-kind condition (the Neumann boundary condition) defined on its boundary:

$$- \sigma_1 \frac{\partial\theta^{(1)}(x)}{\partial \mathbf{n}^{(1)}(x)} = 0, x \in \partial\Omega^{(2)}, \partial\Omega^{(2)} \equiv \partial\Omega = \Gamma_1,$$
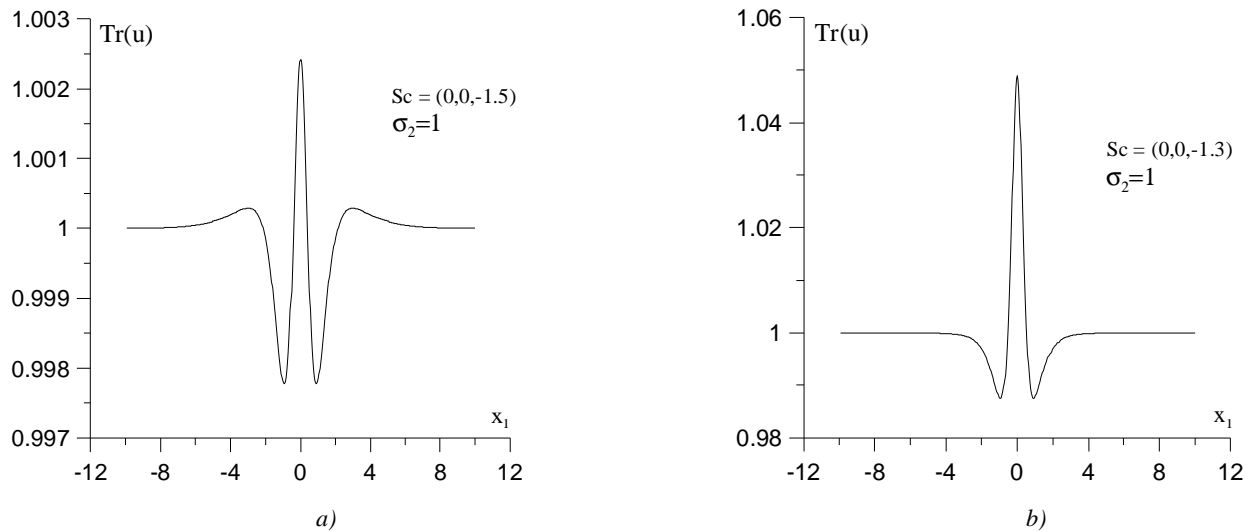
that is the current density equals zero.

Fig. 1. Estimation of a model discretization error (a homogeneous half-space).

The graph in Fig. 1, *b* shows another extreme case, when $\sigma_2 = 1000000$, i.e. the inclusion has a very high conductivity. The curves of the graphs either upward or downward can be understood as follows: in case *a*), the field lines are replaced by a void (an electric current cannot flow here). This results

in the field concentration close to the surface (that is more current flows over the surface) that in turn indicates an increase in the apparent resistivity. In case *b*), the field lines are drawn in by an inclusion of high conductivity (that is a high current flows there), less current flows over the surface. This demonstrates a decrease in the apparent resistivity.
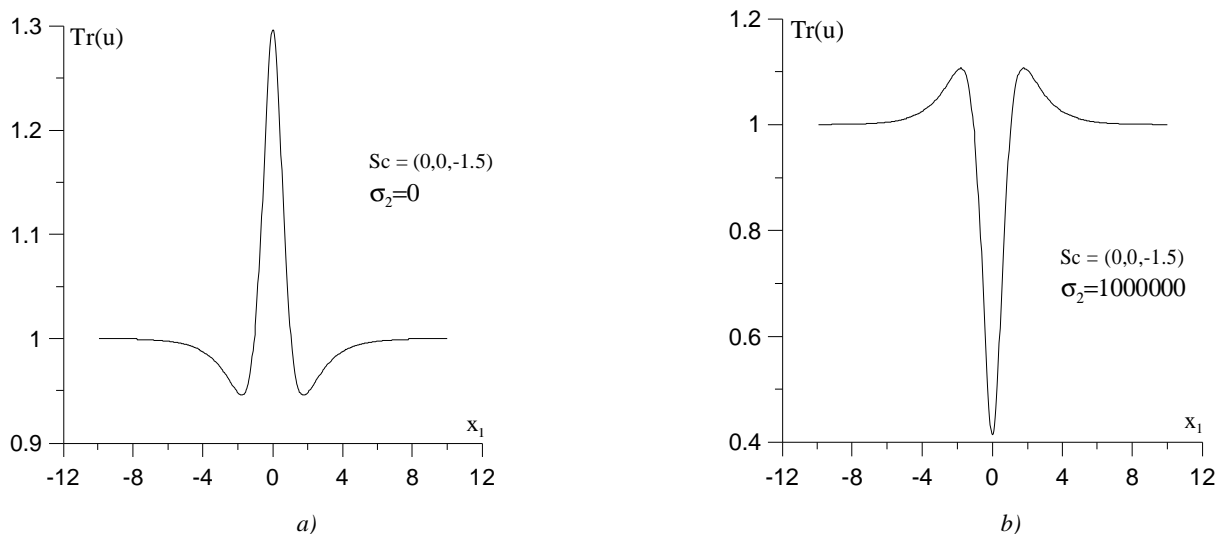
Fig. 2. Estimation of a model discretization error (a – a void with an electrically insulated boundary in a homogeneous half-space; b – a high-conductive inclusion).

Problem 2. *Research into the influence of spherical inclusion conductivity on the apparent resistivity.*

There has beeb done a numerial estimate of the change in the apparent resistivity depending on the inclusion conductivity $\sigma_2 < \sigma_1$ ($\sigma_1 = 1, \sigma_2 = 0.1, 0.2, 0.5, 1$, Fig. 3), and $\sigma_2 > \sigma_1$ ($\sigma_1 = 1, \sigma_2 = 1, 2, 5, 10$, Fig. 4) located at a depth of *H*=1.5. The feeding electrodes were at the points *A*(-10, 0, 0) and *B*(10, 0, 0). As we

can see, as σ_2 grows, the apparent resistivity goes down: even at $\sigma_2 = 10$ the results are slightly different from the limiting case of the superconducting inclusion $\sigma_2=10^6$. The calculations are performed with the optimal number of discretization elements $V = 52$, besause their doubling does not practically influence the accuracy but significantly increases the computation time [10, 11].
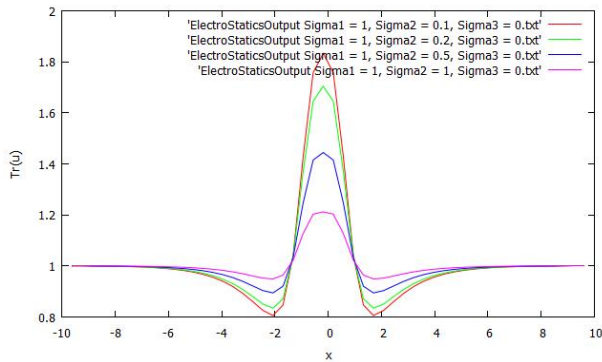
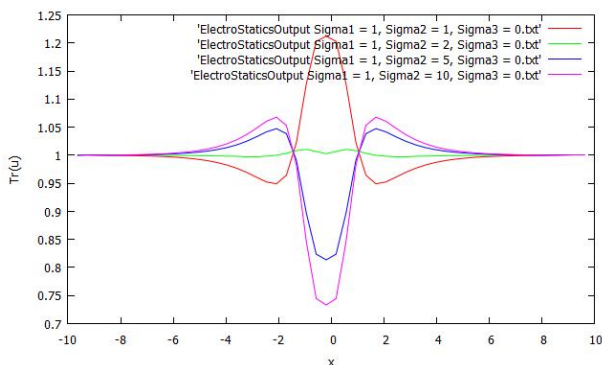*Fig. 3. Apparent resistivity over the high-ohmic inclusion.*

Fig. 4. Apparent resistivity over the conductive inclusion.

As the domain Ω_2 is chosen spherical, the discretization is performed by using a spherical coordinate system. The sphere is divided into meridians and parallels. The "caps" are divided separately into triangular elements of the second order. The "caps'" height is chosen so as to obtain the areas of all the elements approximately equal. The collocation point is selected in the middle of each element. The features in the integrals are identified analytically. The required integrals having been calculated, the Gauss-Jordan method is used for solving SLAEs (36) and (37).

As is obvious, the inclusion is easier to identify at $\sigma_2 > \sigma_1$ rather than at $\sigma_2 < \sigma_1$, because in this case the curves are characterized by a larger value of the maximum that is directly proportional to the value of σ_2.

It is interesting to note that the apparent resistivity deviations from 1 are quite close to the deviations at $s_2 \geq s_1 = 1$ divided by 2, for example

$$Tr(u) \approx 1.3, s_2 = 0, Tr(u) \approx 0.4, s_2 = +\infty$$
$$\Delta Tr(u) \approx 0.3, s_2 = 0, \Delta Tr(u) \approx 0.6, s_2 = +\infty,$$

and also

$$Tr(u) \approx 1.1, s_2 = 0.5, Tr(u) \approx 0.84, s_2 = 2$$
$$\Delta Tr(u) \approx 0.1, s_2 = 0.5, \Delta Tr(u) \approx 0.16, s_2 = 2.$$

Problem 3. *Research into the influence of the inclusion form on the apparent resistivity.*

Spherical inclusions with a radius of R=1, and cube-shaped ones with the length of one side being 2 that are located at a depth of H=1.5 are considered in a half-space with the feeding electrodes at the points A(-20, 0, 0) and B(20, 0, 0). There is a numerical estimate of the change in the apparent resistivity depending on the electrical conductivity and form of inclusion ($\sigma_1 = 1$, $\sigma_2 = 2, 5, 7$, Fig. 5, 6).
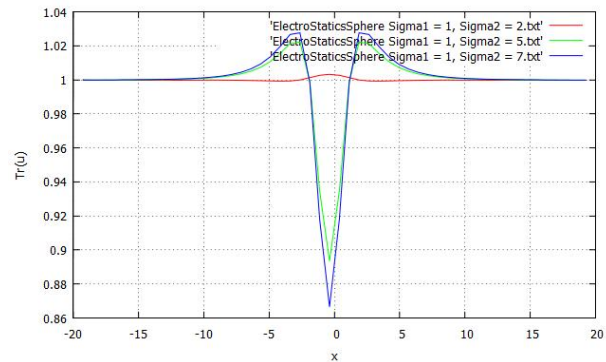

*Fig. 5. Apparent resistivity over
the conductive spherical inclusion.*

As illustrated in Fig. 4 and 5, the apparent resistivity of an inclusion with curved boundaries (which is more common in geoenvironments) is represented by smooth curves. This confirms the necessity to consider nonplanar, but curved boundary elements while developing the discrete models.
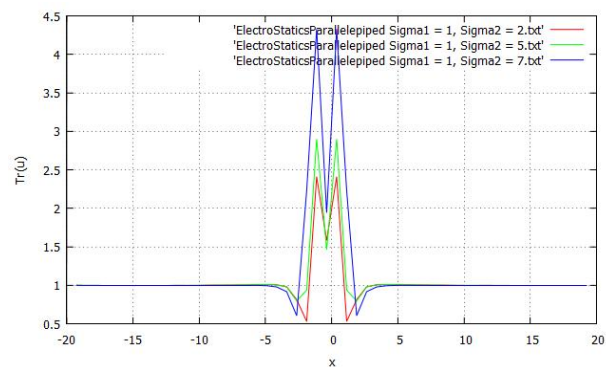

*Fig. 6. Apparent resistivity over the conductive
cube-shaped inclusion.*

The practical implementation of the approach above is considered analyzing the example of an actual problem of surveying and predicting oil and gas deposits, as well as ore ones [9]. The former, as a rule, feature the increased (1,5–4,0 times) electrical resistivity (the quantity inversely proportional to the electrical conductivity) as compared with bearing strata. The latter have a higher electrical conductivity as compared with the bearing strata. For this reason, in the half-space at a

depth of *H,* we choose two similar high-omic or conductive spherical inclusions with a variable distance *d* between them as the simplest model of oil and gas field consisting of two deposits to estimate an electrical profiling resolution by the method of median gradients. This is quite enough to find out the basic regularities of complicated graphs, as increasing the number of inclusions will just cause the appearance of additional repeatable elements.

Problem 4. *Influence of a distance between spherical inclusions on an apparent resistivity.*

Two spherical inclusions with a radius of $R = 1$ and similar conductivity that are located at a depth of $H = 5$ are considered in a half-space with the feeding electrodes at the points $A(-20, 0, 0)$ and $B(20, 0, 0)$.

In case of two inclusions, the SLAE for finding unknown sources introduced into the boundary elements is of the following form:

$$\sum_{v=1}^{V_2+V_3} A_v^{\Gamma 1}(x^{1w},U_h^{(1)})d_v^{\Gamma 1} - \sum_{v=1}^{V_2} A_v^{\Gamma 2}(x^{1w},U^{(2)})d_v^{\Gamma 2} =$$

$$=b^2(x^{1w},U^{(2)}) - b^1(x^{1w},U_h^{(1)}),$$

$$x^{1w} \in \Gamma_2, \ w = 1,...,V_2 , \quad (39)$$

$$\sum_{v=1}^{V_2+V_3} A_v^{\Gamma 1}(x^{1w},U_h^{(1)})d_v^{\Gamma 1} - \sum_{v=1}^{V_3} A_v^{\Gamma 3}(x^{1w},U^{(3)})d_v^{\Gamma 3} =$$

$$=b^3(x^{1w},U^{(3)}) - b^1(x^{1w},U_h^{(1)}),$$

$$x^{1w} \in \Gamma_3, \ w = V_2 +1,...,V_2 + V_3 , \quad (40)$$

$$\sum_{v=1}^{V_2+V_3} A_v^{\Gamma 1}(x^{1w},Q_h^{(1)})d_v^{\Gamma 1} - \sum_{v=1}^{V_2} A_v^{\Gamma 2}(x^{1w},Q^{(2)})d_v^{\Gamma 2} =$$

$$=b^2(x^{1w},Q^{(2)}) - b^1(x^{1w},Q_h^{(1)}),$$

$$x^{1w} \in \Gamma_2, \ w = 1,...,V_2 , \quad (41)$$

$$\sum_{v=1}^{V_2+V_3} A_v^{\Gamma 1}(x^{1w},Q_h^{(1)})d_v^{\Gamma 1} - \sum_{v=1}^{V_3} A_v^{\Gamma 3}(x^{1w},Q^{(3)})d_v^{\Gamma 3} =$$

$$=b^3(x^{1w},Q^{(3)}) - b^1(x^{1w},Q_h^{(1)}),$$

$$x^{1w} \in \Gamma_3, \ w = V_2 +1,...,V_2 + V_3 , \quad (42)$$

where $V_2=V_{12}$, $V_3=V_{13}$.

The calculations are performed with the optimum, in terms of the required accuracy and volume of computing operations, number of discretization elements ($V_1 = V_2 = V_3 = 52$), because their doubling does not influence the accuracy, but significantly increases the computation time.

There is a numerical estimate of the change in the apparent resistivity depending on the distance *d* between

their centres ($d = 2, 6, 10, 20$) ($\sigma_1 = 1, \sigma_2 = \sigma_3 = 0.01$, Fig. 7; $\sigma_1 = 1, \sigma_2 = \sigma_3 = 10$, Fig. 8).

It is shown that at *d/h*=0.25 the graphs of the apparent resistivity ρ_a, calculated by formula (38) do not show any differentiation, and complex heterogeneity is set shown as one high-ohmic inclusion by the maximum of a gradient installation.
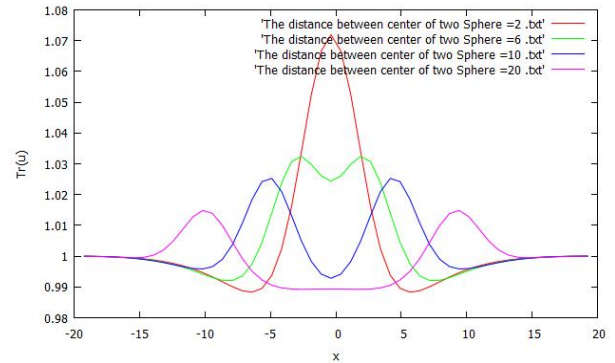

Fig. 7. Apparent resistivity over the two high-ohmic inclusions (dependence on the distance between the centres of inclusions).
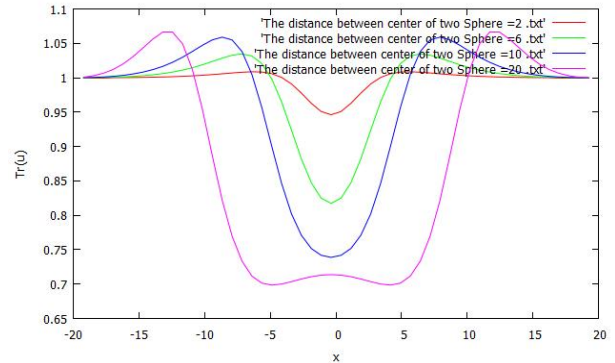

Fig. 8. Apparent resistivity over the two conductive inclusions (dependence on the distance between the centres of inclusions).

Increasing the relative distance between the spheres leads to gradual bifurcation of anomalies on the curves ρ_a, and then to their clear differentiation. So, in simple sections (without screening layers), dc elecrtrical prospecting methods may be successfully used for contouring and dividing high-ohmic oil and gas fields or conductive ore deposits.

Problem 5. *Influence of a spherical inclusions depth on the apparent resistivity.*

Two spherical inclusions with a radius of *R*=1 and similar conductivity that are located at different depths are considered in a half-space with the feeding electrodes at the points *A*(-20, 0, 0) and *B*(20, 0, 0).

There has been performed a numerical estimate of the change in the apparent resistivity depending on a depth H (*H*=1.5, 1.7, 2, 2.5, Fig. 9*)* and electrical conductivity ($\sigma_1 = 1, \sigma_2 = \sigma_3 = 0.5, H = 1.5, 1.7, 2, 2.5$, Fig. 10).

If the inclusions move away from the surface, their influence wanes.This manifests itself in a quantitative decrease in the apparent resistivity value for all σ_2, σ_3. The centres of high-ohmic or conductive inclusions are clearly recorded by the extrema (either maxima or minima) of a gradient installation, with the depth of a model's bed increasing, their value decreases. The anomalies are also smoothed as the size of a receiving line *MN* increases to be optimal.
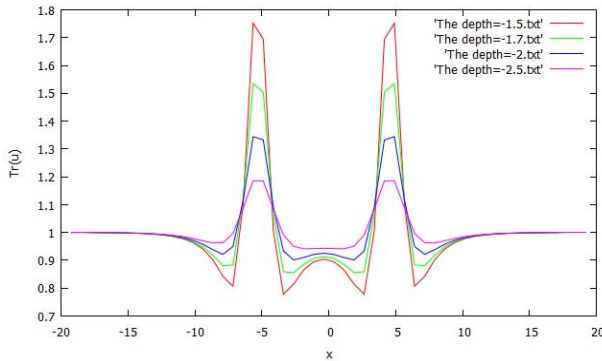

Fig. 9. Apparent resistivity over two high-ohmic
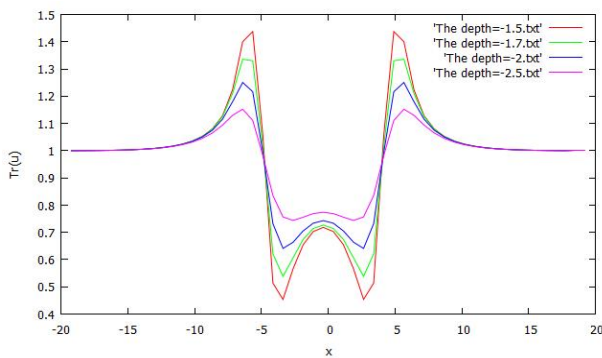$\sigma_1 = 1, \sigma_2 = \sigma_3 = 0.01$ *inclusions (dependence on the depth).*

Fig. 10. Apparent resistivity over two high-ohmic
$\sigma_1 = 1, \sigma_2 = \sigma_3 = 0.5$ *inclusions (dependence on the depth).*

Problem 6. *Influence of the inclusion form on the apparent resistivity.*

Two spherical inclusions with a radius *R*=1 and cube-shaped ones with sides equal to 2 that are located at a depth of *H*=5 with a distance *d=10* between their centres and different conductivity are considered in a half-space with the feeding electrods at the points *A*(-20, 0, 0) and *B*(20, 0, 0). There is a numerical estimate of the change in apparent resistivity depending on the electrical conductivity ($\sigma_1 = \sigma_2 = \sigma_3 = 1$, $\sigma_1 = 1, \sigma_2 = \sigma_3 = 0.01$, $\sigma_2 = 0.01, \sigma_1 = \sigma_3 = 1$, $\sigma_3 = 0.01, \sigma_1 = \sigma_2 = 1$, Fig. 11, Fig. 12).

As we can see, the description of the inclusion boundary by using convex surface areas provides smoother curves of the apparent resistivity which are closer to the real ones.
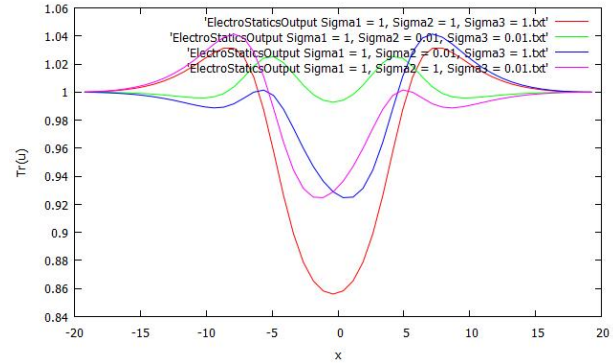

Fig. 11. Apparent resistivity over two high-ohmic spherical inclusions with different electrical conductivity.
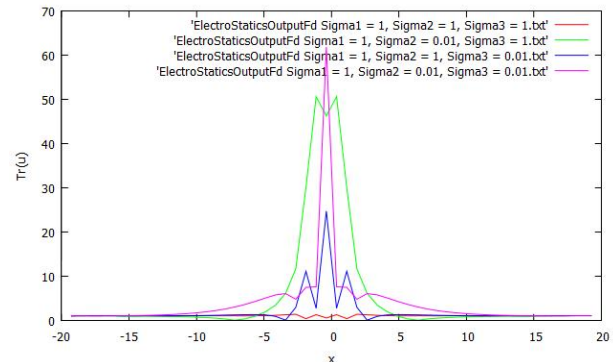

Fig. 12. Apparent resistivity over two high-ohmic cube-shaped inclusions with different electrical conductivity.

7. Conclusion

Errors occurring when using numerical methods for solving such problems are known to be caused by the approximation of equations, contact and boundary conditions, numerical operations of differential and integral calculus. High accurancy of the solutions obtained by means of the techniques suggested is made for by the following factors:

1. Initial equations (1) within homogeneous domains Ω_m, boundary condition (35) are totally satisfied on account of the application of a special fundamental solution.

2. The conditions of potential equality (5) and the conditions of continuity of current density (6) at the media interface are satisfied in a collocation sense. The nonplanar inclusion boundaries are approximated by the quadratic or cubic elements.

3. To achieve the required accuracy, we compare solutions for the different number of boundary and near-boundary elements. The error of satisfying the ideal contact conditions decreases when the number of boundary elements or near-boundary elements increases. However, the complication of a numerical integration procedure (using, for example the allocation of unknown sources within the boundary or near-boundary elements

as continuous functions, but not constant) would significantly reduce the computational errors even with a less number of elements. It should be also noted that the advantages of both approaches consist in the fact that they do not require differentiation of numerical values.

The data above are of fragmentary character, but certain methodical conclusions may be drawn from them.

The results of mathematical modelling and numerical experiments indicate that information on a potential field obtained on the boundary surface and within the object can be used to identify inclusions and determine their conductivity, size and location. The approaches lead to minor errors if the inclusions are located at a distance of not less than 1.5 characteristic dimensions of a receiving source. They can be used to solve direct and inverse problems in different branches of applied mathematics: geophysics, technical diagnostics and testing of materials, in particular when we need to know the distribution of a potential field in objects composed of materials with different characteristics.

Such approaches can become the basis for solving the inverse problems of geophysics and technical diagnostics, in particular to develop methods for the detection of foreign inclusions, and determination of their conductivity, size and location.

The general favourable conditions for the detection and investigation of foreign inclusions with the conductivity either higher or lower than the geoenvironment, should be considered to be a commensurate with lateral /horizontal dimensions (or smaller) depth of their occurrence.

References

[1] L. Zhuravchak and Y. Grytsko, *Near-boundary element technique in applied problems of mathematical physics.* Lviv, Ukraine: Publishing house of Carpathian Branch of Subbotin Institute of Geophysics, NAS of Ukraine, 1996. (Ukrainian)

[2] P. Banerjee and R. Butterfield, *Boundary Element Methods in Engineering Science.* London, UK: McGraw-Hill Book Comp., 1984.

[3] C. Brebbia, J. Telles, and L. Wrobel, *Boundary Element Methods,* Translated from English. Moscow, Russia: Mir, 1987. (Russian)

[4] Y. Zhang, W. Qu, and J. Chen, "A new regularized BEM for 3D potential problems", *Sci Sin Phys Mech Astron*, no. 43, p. 297, 2013.

[5] W. Qu, W. Chen, and Z. Fu, "Solutions of 2D and 3D non-homogeneous potential problems by using a boundary element-collocation method", *Eng Anal Bound Elem*, no. 60, pp. 2–9, 2015.

[6] L. Zhuravchak, B. Grytsko, and O. Kruk, "Numerical and analytical approach to the calculation of thermal fields including thermo sensibility material behavior for complex boundary conditions", *Reports of National Academy of Sciences of Ukraine,* no. 12. pp. 51–57, 2014. (Ukrainian)

[7] L. Zhuravchak and O.Kruk, "Mathematical modeling of distribution of a thermal field in parallelepiped with considering complex heat transfer on its boundary and inner sources", *Kompyuterni nauky ta informatsiyni tekhnologiyi,* no. 771, pp. 291–302, Lviv, Ukraine: Publishing house of Lviv Polytechnic National University, 2013. (Ukrainian)

[8] L. Zhuravchak and N. Shumilina, "Recognition of local volume inhomogeneities for transient thermal field", *Reports of National Academy of Sciences of Ukraine*, no. 10, pp. 42–47, 2005. (Ukrainian)

[9] Ya. S.Sapuzhak and L. Zhuravchak, "The technique of numerical solution of 2-D direct current modeling problem in inhomogeneous media", *Acta Geophysica Polonica*, vol. XLVII, no 2. pp. 149–163, 1999.

[10] L. Zhuravchak and O. Kruk, "Consideration of the nonlinear behavior of environmental material and a three-dimensional internal heat sources in mathematical modeling of heat conduction", *Mathematical modeling and computing*, vol. 2, no. 1, pp. 107–113, 2015.

[11] L. Zhuravchak, O. Kruk, and B. Grytsko, "Mathematical modeling of the distribution of potential field in piecewise homogeneous objects using boundary elements method", in *Proc. XIIIth International Conference "Modern Problems of Radio Engineering, Telecommunications, and Computer Science"*, pp. 117–120, Lviv-Slavsko, Ukraine, February 23–26, 2016.

РОЗВ'ЯЗУВАННЯ ЗАДАЧ ТЕОРІЇ ПОТЕНЦІАЛУ У ТРИВИМІРНИХ КУСКОВО-ОДНОРІДНИХ СЕРЕДОВИЩАХ НЕПРЯМИМИ МЕТОДАМИ ГРАНИЧНИХ І ПРИГРАНИЧНИХ ЕЛЕМЕНТІВ

Любов Журавчак, Олена Крук

Запропоновано ефективні числово-аналітичні методи для розв'язання прямої задачі електророзвідки для середовищ з врахуваннями довільної форми і постійними електричними характеристиками. Вони основані на поєднанні фунда-ментального розв'язку рівняння Лапласа з основними ідеями методів граничних інтегральних рівнянь і колокації.

З використанням непрямих методів граничних і приграничних елементів розвинуто числово-аналітичні

підходи до розв'язання задач теорії потенціалу в просторових кусково-однорідних об'єктах за умов ідеального контакту між їхніми складовими. Дискретно-континуальні моделі для знаходження інтенсивності невідомих джерел, уведених на межі або у зовнішній примежовій області і апроксимованих константами, зведені до систем лінійних алгебраїчних рівнянь. Вони утворюються внаслідок задоволення в колокаційному сенсі крайових умов та умов ідеального контакту.

Здійснено програмну реалізацію запропонованих підходів в півпросторі з врахуваннями різної форми й електропровідності для методу електричного профілювання в задачі електророзвідки постійним струмом Проведені дослідження й отримані числові розв'язки низки математичних моделей ілюструють високу точність і потенційні можливості запропонованих методів. Розроблені алгоритми дають змогу розрахувати потенціал і напруженість електричного поля в неоднорідних середовищах, що характеризуються неплоскими межами включень і довільними за глибиною і латераллю розподілами стаціонарних джерел струму.

Досліджено вплив провідності та глибини включень, їхньої форми, відстані між двома сферичними включеннями на позірний опір, обчислений за значеннями різниці потенціалу, виміряної на поверхні півпростору. Показано, що інформацію про потенціальне поле, одержану на поверхні об'єкта можна використовувати для виявлення в ньому локальних чужорідних включень.

Запропоновані підходи можуть стати основою для розв'язування обернених задач геофізики й технічної діагностики для створення методів розпізнавання чужорідних включень, порожнин і дефектів, визначення їхньої електропровідності, розмірів та місця розташування.

Liubov Zhuravchak. She graduated from Ivan Franko Lviv National University, Faculty of Applied Mathematics and Mechanics in 1985. In 1994 she became Candidate of Physical and Mathematical Sciences, since 2008 she has been Doctor of Technical Sciences.

L. Zhuravchak works at Lviv Polytechnic National University as Professor at the Software Department. Her research interests include mathematical modelling of stationary and non-stationary established processes of thermal conductivity, geoelectricity and linear deformation in two- and three-dimensional piecewise-homogeneous and locally-heterogeneous media of complex form taking into account the dependency of components' properties on coordinates, temperature or strain tensor. Lubov Zhuravchak is the co-author of the near-boundary element method and participates in its further development.

Olena Kruk. She graduated from Ivan Franko Lviv National University, Faculty of Applied Mathematics and Mechanics in 2012. She works at Lviv Polytechnic National University as an assistant professor at the Software Department.

Her research interests include mathematical modelling of stationary processes of the potential theory in three-dimensional piecewise homogeneous objects of complex form whose characteristics depend on the potential.